A Journal of the Gesellschaft Deutscher Chemiker

Angewandte International Edition GDCh Chemie

www.angewandte.org

Accepted Article

Title: Cooperative Catalysis of an Alcohol Dehydrogenase and Rhodium-Modified Periodic Mesoporous Organosilica

Authors: Tomoki Himiyama, Minoru Waki, Yoshifumi Maegawa, and Shinji Inagaki

To be cited as: *Angew. Chem. Int. Ed.* 10.1002/anie.201904116
Angew. Chem. 10.1002/ange.201904116

Link to VoR: http://dx.doi.org/10.1002/anie.201904116
http://dx.doi.org/10.1002/ange.201904116

WILEY-VCH

10.1002/anie.201904116

WILEY-VCH

Cooperative Catalysis of an Alcohol Dehydrogenase and Rhodium-Modified Periodic Mesoporous Organosilica

*Tomoki Himiyama, Minoru Waki, Yoshifumi Maegawa, and Shinji Inagaki**

Abstract: The combined use of a metal complex catalyst and an enzyme is an attractive concept, but typically results in mutual inactivation. A rhodium (Rh) complex immobilized in a bipyridine-based periodic mesoporous organosilica (BPy-PMO) shows high catalytic activity during transfer hydrogenation in the presence of a model protein, bovine serum albumin (BSA), while a homogeneous Rh complex exhibits reduced activity due to direct interaction with the BSA. The use of a smaller protein or an amino acid instead of BSA revealed a clear size-sieving effect of the BPy-PMO that protected the Rh catalyst from direct interactions. A combination of Rh-immobilized BPy-PMO and an enzyme (horse liver alcohol dehydrogenase; HLADH) successfully promoted sequential reactions involving the transfer hydrogenation of NAD^+ to give NADH followed by the asymmetric hydrogenation of 4-phenyl-2-butanone based on the generation of NADH with high enantioselectivity. This result indicates the significant compatibility of Rh-immobilized BPy-PMO with HLADH. The use of BPy-PMO as a support for metal complexes could potentially be applied to various other systems consisting of a metal complex catalyst and an enzyme.

Combinations of metal complex catalysts with enzymes are expected to provide a new approach to achieving unique chemical transformations.[1] Artificial metal complexes can exhibit catalytic activities that are rarely obtained from natural enzymes, while enzymes can allow highly selective catalysis. One approach for their combination is direct linkage of transition metal ions to protein surfaces to form hybrid biocatalysts, which showed high enantioselectivity for the reactions missing from nature's toolbox.[2] Another approach is using both a metal complex and an enzyme simultaneously to achieve one-pot cascade reactions in sequential steps. This approach is interesting but a crucial issue for the combined use due to the mutual inactivation of metal complexes and enzymes via nonspecific interactions (Figure 1a). Several strategies have been developed to overcome this problem and enable the combined use of metal complexes and enzymes, based on compartmentalization.[3]

Mesoporous materials having uniform pores with nano-scale diameters should exclude proteins larger than the pore diameters. Taking advantage of this size-sieving effect, direct interactions between a protein and a metal complex can be avoided by locating the complex inside the mesopores. As an example, an oxovanadium complex immobilized on the pore surfaces of mesoporous silica was used together with lipase for the dynamic kinetic resolution of racemic alcohols.[4] The size-sieving effect of the mesopores improved the compatibility of the metal complex and the lipase, indicating that the undesired interaction between the vanadium catalytic center and the enzyme were reduced. Developing a mesoporous support capable of forming a variety of metal complexes on its pore surfaces would allow the simultaneous use of a wide variety of metal complex catalysts and proteins.

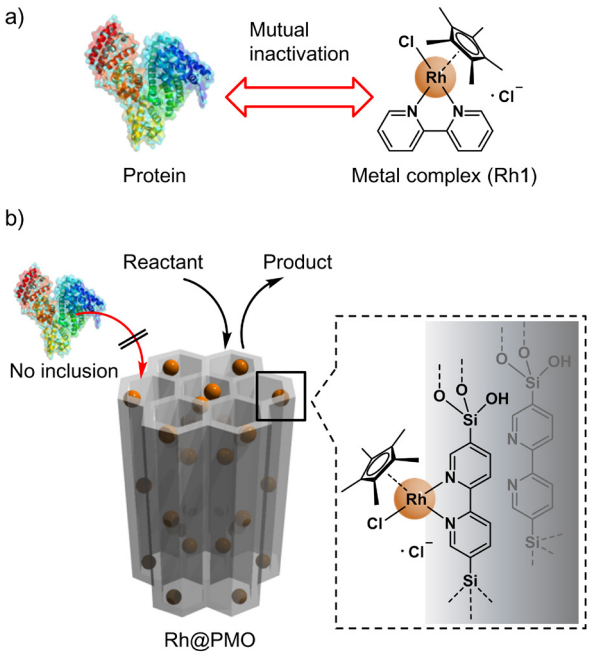

Figure 1. (a) Mutual inactivation between a protein and a metal complex. (b) A schematic representation of Rh@PMO. The rhodium catalytic centers inside the mesopores are protected via the size-sieving effect to avoid inactivation by the protein.

Recently, we reported a periodic mesoporous organosilica (PMO) containing 2,2'-bipyridine (BPy) ligands densely packed on the pore surfaces (BPy-PMO).[5a] In this material, the BPy groups can function as bidentate ligands for many different metal complexes. To date, a variety of metal complexes have been formed on these ligands, to obtain materials such as Ir(cod)(OMe)(BPy) (cod: 1,5-cyclooctadiene), $[Ru(bpy)_2(BPy)]^{2+}$ (bpy: 2,2'-bipyridine), $RuCl_2(CO)_2(BPy)$, $[IrCp^*Cl(BPy)]^+$ (Cp^*: pentamethylcyclopentadiene), $Re(CO)_3Cl(BPy)$ and $MoO_2Cl(OH)(BPy)$.[5] These immobilized metal complexes on the BPy-PMO have exhibited efficient heterogeneous catalysis because

[*] Dr. T. Himiyama, Dr. M. Waki, Y. Maegawa, Dr. S. Inagaki
Toyota Central R&D Laboratories, Inc.
Nagakute, Aichi 480-1192 (Japan)
E-mail: inagaki@mosk.tytlabs.co.jp
Dr. T. Himiyama
Current address : National Institute of Advanced Industrial Science and Technology, Ikeda, Osaka 563-8577 (Japan)

Supporting information for this article is given via a link at the end of the document.

of the formation of the isolated metal complex center on the well-defined pore surface and the ready diffusion of molecules in the large pores (3.8 nm in diameter). Non-enzymatic regeneration of NADH have been developed by using Rh catalysts such as [RhCp*(bpy)Cl]Cl (Rh**1**).[6] Hydride transfer takes place via key intermediate of rhodium hydride complex in the formate-driven mechanism, which was well investigated in previous literatures.[7] The NADH drives an enzyme to catalyze an enantioselective transformation. However, the Rh-complex catalyst is known to strongly interact with proteins, leading to mutual inactivation, meaning that a sequential reaction based on the combined use of this catalyst and an enzyme is very difficult or impossible.[1c,8]

Here, we report the catalytic performance of Rh-immobilized BPy-PMO (Rh@PMO) in the presence of a protein, as well as the cooperative catalysis of an enzyme and Rh@PMO (Figure 1b). Rh@PMO was found to exhibit high catalytic activity during transfer hydrogenation even in the presence of a protein having a molecular size larger than the pore diameter, indicating the ability to tolerate a large protein. The combined use of Rh@PMO and an enzyme promoted sequential reactions consisting of the transfer hydrogenation of NAD^+ to NADH as well as asymmetric hydrogenation using NADH with high conversion and good enantioselectivity, indicating the compatibility of the Rh@PMO and the enzyme.

Rh@PMO was prepared by mixing $[RhCp^*Cl_2]_2$ and BPy-PMO powder in MeOH according to a previously reported technique, with some modifications.[9] The use of MeOH instead of DMF preserved the highly ordered mesoporous structure of the PMO after immobilization of the Rh complex. Complexation of the Rh was confirmed by UV-vis diffuse reflectance spectroscopy, X-ray absorption fine structure spectroscopy (XAFS) and energy-dispersive X-ray spectroscopy (EDX). The UV-vis spectrum of the Rh@PMO contained a characteristic absorption band at 380 nm, attributed to the formation of $[RhCp^*(bpy)Cl]^+$ on the pore surfaces (Figure S1). X-ray absorption near-edge spectroscopy (XANES) and extended X-ray absorption fine structure (EXAFS) Fourier transform analysis at the Rh *K*-edge of the Rh@PMO generated data similar to those obtained from Rh**1**. This result indicates that the oxidation states and coordination symmetries of the Rh centers in the Rh@PMO and Rh**1** were similar (Figure S2). Curve-fitting analysis of the Rh *K*-edge EXAFS Fourier transforms also demonstrated that both materials had a similar local coordination structure (Figure S3 and Table S1 for curve fitting). The EDX analysis of the Rh@PMO showed that the molar proportion of Rh relative to BPy was 6.3%, which corresponds to a concentration of the Rh complex in the BPy-PMO of 0.22 mmol g^{-1} (BPy: 3.18 mmol g^{-1}). The EDX maps acquired from the Rh@PMO indicated that the Rh atoms were homogeneously distributed over the PMO particles as well as over the Si atoms (Figure S4).

The XRD pattern of the Rh@PMO presented low angle reflections at 2θ values of 1.82°, 3.18° and 4.85° due to the two-dimensional hexagonal lattice. Three additional peaks were also present at scattering angles of 7.60°, 15.6° and 23.0° as a result of the molecular-scale periodicity of the bipyridine groups inside the pore walls. These results confirm that the original structure of the BPy-PMO was preserved even after immobilization of the Rh complex on the pore surfaces (Figure S5). The nitrogen adsorption/desorption isotherms generated by the Rh@PMO were identified as type-IV, similar to those obtained from the pristine BPy-PMO (Figure S6). Density functional theory pore diameter (D_{DFT}), Brunauer-Emmett-Teller surface area (S_{BET}) and t-plot pore volume ($V_{t\text{-}plot}$) values were derived from the isotherms and are summarized in Table 1. All three values were slightly reduced following immobilization of the Rh complex, suggesting the formation of Rh complexes in the mesopores of the BPy-PMO.

The catalytic activities of the homogeneous material Rh**1** and of Rh@PMO were evaluated during the transfer hydrogenation of 2-cyclohexen-1-one in the presence of BSA as a model protein (Scheme 1). The homogeneous Rh**1** showed high catalytic activity, affording cyclohexanone in almost 100% yield after 1.3 h in the absence of BSA (Figure S7a). However, the addition of BSA to the homogeneous reaction solution drastically reduced the activity due to the deactivation of the Rh**1** via nonspecific interactions with the BSA protein. The Rh@PMO also exhibited good catalytic activity for this reaction in the absence of BSA, although the reaction rate was lower than that of the homogeneous Rh**1** (Figure S7b). Interestingly, the activity of the Rh@PMO was not greatly reduced when BSA was added. The catalytic activity was likely retained because the Rh catalyst in the PMO was not deactivated by the BSA, as this large protein (14 × 4 × 4 nm, 66 kDa) could not enter the mesopores (which had a diameter of 3.7 nm). Hot filtration experiments demonstrated that the Rh complex was strongly bound to the Rh@PMO and thus was not leached out during the reaction either in the absence or presence of BSA (Figure S8).

Table 1. Physicochemical properties of BPy-PMO and Rh@PMO.

Material	S_{BET}[a] / m^2 g^{-1}	D_{DFT}[b] / nm	$V_{t\text{-}plot}$[a] / cm^3 g^{-1}
BPy-PMO	600	4.3	0.34
Rh@PMO	430	3.7	0.27

[a] Determined from the adsorption branches of the isotherms. [b] Determined from the desorption branches of the isotherms.

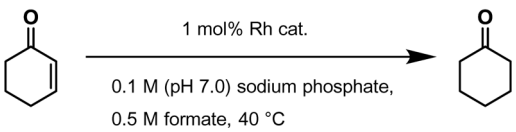

Scheme 1. Transfer hydrogenation of 2-cyclohexen-1-one by a rhodium catalyst.

Figure 2 plots the conversions after 6 h as functions of the BSA concentration for various catalysts. The conversion over the homogeneous Rh**1** decreased significantly with increases in the BSA concentration, while the Rh@PMO maintained a high level

of conversion (over 80%) even at BSA concentrations up to 20 mg mL^{-1}. This result shows the superior ability of the Rh@PMO to tolerate the presence of the BSA protein. We also examined the tolerance properties obtained with another mesoporous silica solid support (FSM-16) and with silica gel. The Rh-complex catalyst was grafted onto the surfaces of the FSM-16 and silica gel using a molecular linker, to afford Rh@FSM-16 and Rh@SilicaGel (Scheme S1). These supported Rh-complex catalysts also demonstrated continued high levels of activity in the presence of BSA (Figure 2). This occurred because the FSM-16 and silica gel had pore diameters (4.7 and 5.4 nm, respectively) that were smaller than the molecular size of the BSA. However, the catalytic activity of the Rh@PMO was higher than those of the Rh@FSM-16 and Rh@SilicaGel in the absence or presence of BSA. The direct immobilization of the Rh complex on the pore surfaces without a linker when using the Rh@PMO is evidently advantageous in terms of preserving the original activity of the homogeneous Rh**1** catalyst, as has been reported previously.[5]

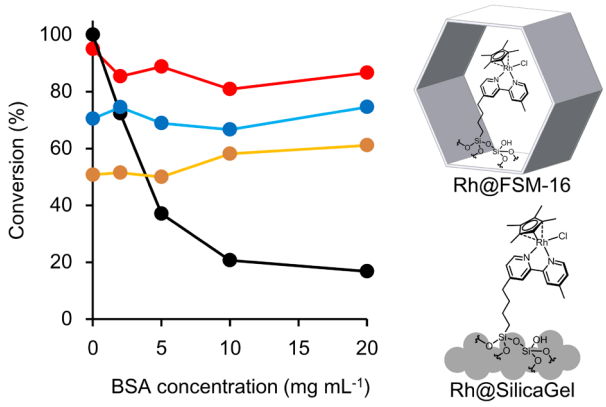

Figure 2. Conversions of 2-cyclohexen-1-one after 6 h in the presence of BSA (0-20 mg mL^{-1}). Catalyst; Rh**1** (black), Rh@PMO (red), Rh@FSM-16 (yellow) and Rh@SilicaGel (blue).

To further investigate the size-sieving ability of Rh@PMO, a small protein, myoglobin (Mb, with a molecular size of 2 × 3 × 4 nm), and an amino acid, histidine (His), were used instead of BSA (Figure 3). The addition of His almost completely quenched the transfer hydrogenation reaction when using either Rh@PMO or homogeneous Rh**1** as the catalyst because the small His molecules were able to enter the mesopores and coordinate with the Rh complex to inactivate the catalyst. The addition of Mb almost fully stopped the reaction in the case of the Rh**1**, although the Rh@PMO catalyst retained some activity because the Mb molecules are almost equal in size to the Rh@PMO pores. These results clearly indicate the size-sieving property of the Rh@PMO.

Next, we investigated the sequential reactions involved in the combined use of Rh@PMO and enzyme (Scheme 2). Horse liver alcohol dehydrogenase (HLADH) is known to catalyze the asymmetric hydrogenation of 4-phenyl-2-butanone in the presence of NADH.[7,10] In addition, Rh**1** catalyzes the transfer hydrogenation of NAD$^+$ to NADH in the presence of formate as a hydride donor.[5] Thus, the asymmetric hydrogenation of 4-phenyl-2-butanone was promoted by a mixture of Rh catalysts and HLADH in conjunction with NAD$^+$ and formate (Figure S9). The combination of homogeneous Rh**1** and HLADH gave the corresponding alcohol, (*S*)-(+)-4-phenyl-2-butanol, with a 71% conversion and 96% ee after 20 h (entry 1 in Table 2). After a 42 h reaction, the conversion was improved to 80% but the enantioselectivity was decreased to 87% ee (entry 2 in Table 2). A precipitate was observed to form in the reaction solution after 20 h and the UV-vis spectrum of the supernatant of the reaction solution showed no absorption that could be attributed to HLADH (Figure S10). These results suggest that the HLADH was deactivated due to its interaction with the Rh**1** catalyst during the reaction. Actually, the considerable amount of Rh was detected in the precipitate by inductively coupled plasma (ICP)-atomic emission spectrometry (AES) (Supporting Information). The decrease in enantiomeric purity with time is attributed to the deactivation of the HLADH and the subsequent formation of a racemic product by the Rh**1** because the Rh**1** alone generates racemic 4-phenyl-2-butanol (entry 3 in Table 2).

The combined use of Rh@PMO and HLADH afforded the corresponding alcohol in 69% conversion with >97% ee after 20 h (entry 4 in Table 2) and 91% conversion with a higher enantioselectivity of >98% ee after 42 h (entry 5 in Table 2). The UV-vis spectrum of the reaction solution after 20 h exhibited a characteristic absorption band at 280 nm due to HLADH (Figure S10), suggesting that HLADH was still active and capable of generating the enantiomeric product even after 20 h. It is therefore evident that the Rh catalyst in the pores of PMO was protected from the direct interaction with the HLADH because the pore diameters were smaller than the HLADH (10 × 6 × 4 nm).

Rh@PMO played a role in regeneration of cofactor NADH from NAD$^+$, which was confirmed by the experiment using no HLADH (Figure S11). The regeneration efficiency was evaluated by total turnover number (TTN), which was defined as mole product per mole cofactor, in the combined reaction system of Rh@PMO and HLADH. TTN were 2.4 – 5.7, which was not so high but indicated the regeneration of NADH in the combined reaction system (Table S2).

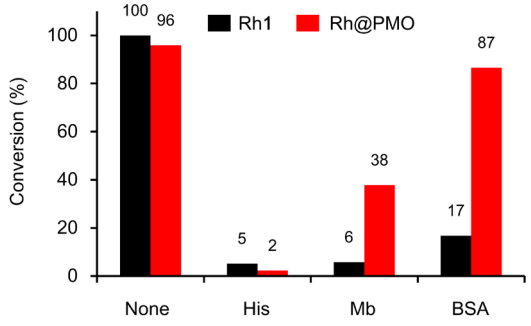

Figure 3. Conversions of 2-cyclohexen-1-one after 6 h in the absence (None) and presence of His (2.0 mg mL^{-1}), Mb (20 mg mL^{-1}) or BSA (20 mg mL^{-1}). Catalyst; Rh**1** (black), Rh@PMO (red).

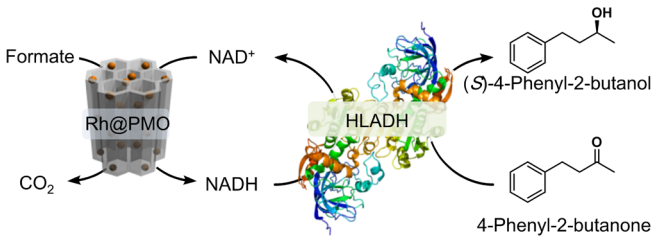

Scheme 2. Asymmetric hydrogenation by combining Rh@PMO and HLADH.

Table 2. Asymmetric hydrogenation of 4-phenyl-2-butanone.

Entry	Catalyst	Reaction time [h]	Conversion [%]	ee [%][a]
1	Rh**1**	20	71	96
2	Rh**1**	42	80	87
3[b]	Rh**1**	42	95	0
4	Rh@PMO	20	69	>98
5	Rh@PMO	42	91	>98
6	Rh@FSM-16	20	60	>98
7	Rh@FSM-16	42	71	>98
8	Rh@SilicaGel	20	65	92
9	Rh@SilicaGel	42	71	88
10[c]	Rh@PMO	20	99	97

[a] Positive ee indicates preferential formation of (*S*)-(+)-4-phenyl-2-butanol. [b] The reaction was conducted without HLADH. [c] The reaction was carried out with $NADP^+$ and NADPH-dependent ADH instead of NAD^+ and HLADH.

Rh@FSM-16 and Rh@SilicaGel were also examined with regard to the asymmetric hydrogenation in combination with HLADH. The Rh@FSM-16 gave a high enantioselectivity of >98%, similar to the Rh@PMO, but a lower conversion of 71% after a 42 h reaction (entries 6-7 in Table 2). This high enantioselectivity indicates that the FSM-16 also prevented deactivation of the HLADH. However, the low conversion confirms the reduced catalytic activity of the Rh complex when immobilized on FSM-16 compared to BPy-PMO, as noted earlier. The Rh@SilicaGel exhibited a low conversion of 71% together with a relatively poor enantioselectivity of 88% ee after 42 h (entries 8-9 in Table 2). The UV-vis spectrum showed that the HLADH still remained in the solution after the reaction (Figure S10). Therefore, the decrease in enantioselectivity could have been caused by an undesirable interaction between the HLADH and the silica gel, which had a disordered structure. The low conversion is attributed to the poor activity of the Rh complex when immobilized on silica gel. These results demonstrate that BPy-PMO is an excellent support for the Rh complex and not only prevents deactivation of the HLADH but also preserves the high activity of the original Rh catalyst.

The principle of the combined use of Rh@PMO and HLADH was also demonstrated for NADPH-dependent enzyme. Rh@PMO also catalyzed reduction of $NADP^+$ to NADPH in the presence of formate (Figure S12). The mixture of Rh@PMO and NADPH-dependent enzyme in conjunction with NADPH and formate successfully catalyzed the asymmetric hydrogenation of 4-phenyl-2-butanone, giving the corresponding alcohol in 99% conversion with 97% ee after 20 h (entry 10 in Table 2, and Figures S12 and S13).

In conclusion, Rh@PMO shows high catalytic activity and significant tolerance to the presence of BSA during the transfer hydrogenation of 2-cyclohexen-1-one. The additions of His or Mb in place of BSA completely or partly quench the reaction when using Rh@PMO, demonstrating the size-sieving effect of the PMO. A one-pot reaction involving the initial formation of NADH followed by asymmetric hydrogenation using the NADH was successfully performed by combining Rh@PMO and HLADH. The reaction gave high conversion and enantioselectivity due to the compatibility of the two materials. This method could be expanded for use with a variety of one-pot reactions based on mixtures of metal complex-immobilized BPy-PMO and enzymes.

Experimental Section

Hydrogenation of 2-cyclohexen-1-one. The reactions were performed at 40 °C in a 0.10 M (pH 7.0) sodium phosphate buffer solution (2.0 mL) containing 0.5 M formate, the Rh catalyst (0.20 μmol) and 2-cyclohexen-1-one (20 μmol) as the substrate. The reaction mixture (100 μL) was subsequently collected and extracted with ethyl acetate (500 μL) three times. The organic phase was analyzed by gas chromatography using phenol as an internal standard.

Asymmetric hydrogenation of 4-phenyl-2-butanone using HLADH. The reactions were carried out at 40 °C in a 0.10 M (pH 7.0) sodium phosphate buffer solution (2.0 mL) containing 0.1 M formate, NAD^+ (3.0 μmol), the Rh catalyst (0.60 μmol), HLADH (2.5 mg, 5 U) and 4-phenyl-2-butanone (8.0 μmol) as the substrate. The reaction mixture (500 μL) was subsequently collected and extracted with ethyl acetate (500 μL) three times. The organic phase was analyzed by gas chromatography using phenol as an internal standard.

Asymmetric hydrogenation of 4-phenyl-2-butanone using NADPH-dependent ADH. The reactions were carried out at 40 °C in a 0.10 M (pH 7.0) sodium phosphate buffer solution (2.0 mL) containing 0.1 M formate, $NADP^+$ (3.0 μmol), the Rh catalyst (0.60 μmol), NADPH-dependent ADH (4 U) and 4-phenyl-2-butanone (8.0 μmol) as the substrate. The reaction mixture (500 μL) was subsequently collected and extracted with ethyl acetate (500 μL) three times. The organic phase was analyzed by gas chromatography using phenol as an internal standard.

Acknowledgements

We thank Dr. Masamichi Ikai, Dr. Yasutomo Goto and Mr. Satoshi Kosaka of Toyota Central R&D Labs. Inc. for performing

the XAFS, TEM and ICP-AES analyses, respectively. The XAFS work was performed at SPring-8 (BL14B2: proposals 2016B1617 and 2017A1822). This work was supported by JST ACT-C, Japan (JPMJCR12Y1).

Conflict of interest

The authors declare no conflict of interest.

Keywords: rhodium • mesoporous materials • heterogeneous catalysis • hydrogenation • enzyme catalysis

[1] a) F. Rudroff, M. D. Mihovilovic, H. Gröger, R. Snajdrova, H. Iding, U. T. Bornscheuer, *Nat. Catal.* **2018**, *1*, 12-22; b) Y. Wang, H. Zhao *Catalysis*, **2016**, *6*, 194; c) C. A. Denard, J. F. Hartwig, H. Zhao, *ACS Catal.* **2013**, *3*, 2856-2864; d) M. J. Kim, Y. I. Chung, Y. K. Choi, H. K. Lee, D. Kim, J. Park, *J. Am. Chem. Soc.* **2003**, *125*, 11494-11495; e) B. Martín-Mature, M. Edin, K. Bogár, J. Bäckvall, *Angew. Chem.* **2004**, *116*, 6697-6701; *Angew. Chem. Int. Ed.* **2004**, *43*, 6535-6539; f) C. A. Denard, M. J. Bartlett, Y. Wang, L. Lu, J. F. Hartwig, H. Zhao, *ACS Catal.* **2015**, *5*, 3817-3822; g) G. Gonzalo, G. Ottolina, G. Carrea, M. W. Fraaije, *Chem. Commun.* **2005**, 3724-3726.

[2] a) Q. Jing, K. Okrasa, R. J. Kazlauskas, *Chem. Eur. J.* **2009**, *15*, 1370-1376; b) K. Okrasa, R. J. Kazlauskas, *Chem. Eur. J.* **2006**, *12*, 1587-1596.

[3] a) Z. J. Wang, K. N. Clary, R. G. Bergman, K. N. Raymond, F. D. Toste, *Nat. Chem.* **2013**, *5*, 100-103; b) H. Sato, W. Hummel, H. Gröger, *Angew. Chem.* **2015**, *127*, 4570-4574; *Angew. Chem. Int. Ed.* **2015**, *54*, 4488-4492; c) Á. G. Baraibar, D. Reichert, C. Mugge, S. Seger, H. Gröger, R. Kourist, *Angew. Chem.* **2016**, *128*, 15043-15047; *Angew. Chem. Int. Ed.*, **2016**, *55*, 14823-14827; d) V. Köhler, Y. M. Wilson, M. Dürrenberger, D. Ghislieri, E. Churakova, T. Quinto, L. Knorr, D. Häussinger, F. Hollmann, N. J. Turner, T. R. Ward, *Nat. Chem.*, **2013**, *5*, 93-99; e) Y. Okamoto, V. Köhler, T. R. Ward, *J. Am. Chem. Soc.* **2016**, *138*, 5781-5784; f) Y. Okamoto, V. Kohler, C. E. Paul, F. Hollmann, T. R. Ward, *ACS Catal.*, **2016**, *6*, 3553-3557;

[4] a) M. Egi, K. Sugiyama, M. Saneto, R. Hanada, K. Kato, S. Akai, *Angew. Chem.* **2013**, *125*, 3742-3746; *Angew. Chem. Int. Ed.*, **2013**, *52*, 3654-3658; b) K. Sugiyama, Y. Oki, S. Kawanishi, K. Kato, T. Ikawa, M. Egi, S. Akai, *Catal. Sci. Technol.*, **2016**, *6*, 5023-5030.

[5] a) M. Waki, Y. Maegawa, K. Hara, Y. Goto, S. Shirai, Y. Yamada, N. Mizoshita, T. Tani, W. Chun, S. Muratsugu, M. Tada, A. Fukuoka, S. Inagaki, *J. Am. Chem. Soc.* **2014**, *136*, 4003-4011; b) N. Ishito, H. Kobayashi, K. Nakajima, Y. Maegawa, S. Inagaki, K. Hara, A. Fukuoka, *Chem. Eur. J.* **2015**, *26*, 15564-15569. c) X. Liu, Y. Maegawa, Y. Goto, K. Hara, S. Inagaki, *Angew. Chem.* **2016**, *128*, 8075-8079; *Angew. Chem. Int. Ed.* **2016**, *55*, 7943-7947; d) Y. Maegawa, S. Inagaki, *Dalton Trans.* **2015**, *44*, 13007-13016; e) M. Waki, K. Yamanaka, S. Shirai, Y. Maegawa, Y. Goto, Y. Yamada, S. Inagaki, *Chem. Eur. J.* **2018**, *24*, 3846-3853; f) S. Ishikawa, Y. Maegawa, M. Waki, S. Inagaki, *ACS Catal.* **2018**, *8*, 4160-4169.

[6] a) L. Zhang, R. Qiu, X. Xue, Y. Pan, C. Xu, H. Li, L. XU, *Adv. Synth. Catal.* **2015**, *357*, 3529-3537; b) K. T. Oppelt, E. Wöβ, M. Stiftinger, W. Schöfberger, W. Buchberger, G. Knör, *Inorg. Chem.*, **2013**, *52*, 11910-11922; c) K. T. Oppelt, J. Gasiorowski, D. A. M. Egbe, J. P. Kollender, M. Himmelsbach, A. W. Hassel, N. S. Sariciftci, G. Knör, *J. Am. Chem. Soc.* **2014**, *136*, 12721-12729; d) C. L. Pitman, O. N. L. Finster, A. J. M. Miller, *Chem. Commun.*, **2016**, *52*, 9105−9108.

[7] V. D. Westerhausen, S. Herrmann, W. Hummel, E. Steckhan, *Angew. Chem.* **1992**, *104*, 1496-1498; *Angew. Chem. Int. Ed. Engl.* **1992**, *31*, 1529-1531.

[8] a) F. Hildebrand, S. Lütz, *Chem. Eur. J.*, **2009**, *15*, 4998-5001; b) M. Poizat, I. W. C. E. Arends, F. Hollmann, *J. Mol. Catal. B: Enzym.* **2010**, *63*, 149-156.

[9] K. Matsui, Y. Maegawa, M. Waki, S. Inagaki, Y. Yamamoto, *Catal. Sci. Technol.* **2018**, *8*, 534-539.

[10] H. C. Lo, R. H. Fish, *Angew. Chem.* **2002**, *114*, 496-499; *Angew. Chem. Int. Ed.*, **2002**, *41*, 478-481.

10.1002/anie.201904116

WILEY-VCH

Entry for the Table of Contents

COMMUNICATION

A rhodium complex immobilized in a bipyridine-based periodic mesoporous organosilica, Rh@PMO, exhibited high catalytic activity during transfer hydrogenation in the presence of a protein, indicating excellent tolerance for the protein due to the size-sieving effect of the PMO. A mixture of Rh@PMO and an alcohol dehydrogenase promoted sequential reactions to afford an enantiomeric product with high conversion and enantioselectivity.

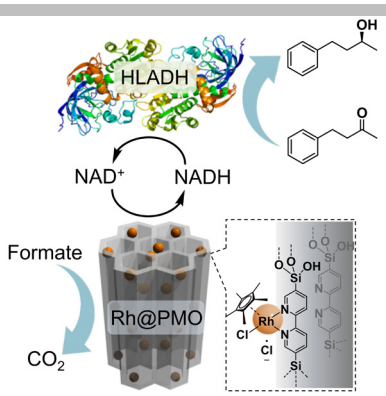

*Tomoki Himiyama, Minoru Waki, Yoshifumi Maegawa, and Shinji Inagaki**

Page No. – Page No.

Cooperative catalysis of an alcohol dehydrogenase and rhodium-modified periodic mesoporous organosilica